

Validation of prestressed concrete high-fidelity finite element analysis

Aaron Freidenberg, Lyle R. Milliman, Benjamin Parmer, Gbenga Olaolorun, Evan Pape, and Bradley Durant

- Building on design principles from PCI's Engineering Student Design Competition, also known as the Big Beam Contest, this paper presents a finite element analysis of prestressed concrete beams subjected to dynamic loading.
- Computer modeling was completed for four prestressed concrete beam configurations.
- Laboratory testing was also completed for each of the four beam configurations to compare the predicted and experimental results and validate the proposed methodology.

High-fidelity finite element analysis simulations of prestressed concrete beams are becoming increasingly common for situations that involve extreme load cases, such as blast or seismic loading. The use of unconventional beam materials and/or geometries may also necessitate such an analysis. While prestressed concrete beam behavior in the uncracked, elastic range can be easily handled using analytical formulas, beyond the first concrete tension crack the behavior becomes significantly more complex.

Beyond the first crack, which occurs well before the steel prestressing strands yield, the beam behavior (for example, load-deflection relation) becomes very difficult to predict analytically. This is because as the tension crack propagates, it shifts the location of the neutral axis and causes a reduction in the effective moment of inertia. Steel prestressing strand (for example, 0.5 in. [12.7 mm] special) is also highly ductile, and the beam will have significant additional capacity beyond first yield. Beam behavior in this post-yielding regime, deflections in particular, are difficult to predict. In addition, for many extreme load cases—such as seismic, blast, and impact loading—dynamic effects must be considered.

This paper presents a methodology for simulating pretensioning using a finite element analysis program. Although the focus is on detailed quasistatic displacement control beam behavior using an explicit dynamic analysis method, the method can be used for any geometry under any loading. The material

PCI Journal (ISSN 0887-9672) V. 64, No. 5, September–October 2019.

PCI Journal is published bimonthly by the Precast/Prestressed Concrete Institute, 200 W. Adams St., Suite 2100, Chicago, IL 60606.

Copyright © 2019, Precast/Prestressed Concrete Institute. The Precast/Prestressed Concrete Institute is not responsible for statements made by authors of papers in *PCI Journal*. Original manuscripts and discussion on published papers are accepted on review in accordance with the Precast/Prestressed Concrete Institute's peer-review process. No payment is offered.

model for the concrete includes a fracture energy parameter to simulate crack propagations along with a standard plasticity model for the reinforcing steel and strands. Full-scale experiments were performed to validate all models. The method is easily extended to transient dynamic loads, as will be discussed.

The simplest method for pretensioning in the finite element software program is to assume a prestressing force in the prestressing strand that is constant along the length of the strand, as well as constant from the start time until the simulation's termination time. This method, which is explained in detail by Bojanowski and Balcerzak,¹ has the advantage of being a simple method that it is easy to implement. The disadvantage is a lack of accuracy because consideration of the yielding of the prestressing strands is not possible using this method. Variation of prestressing force along the length of the strand is also not considered. This causes a number of issues, most notably that the pretensioning forces are much too high at the supports, resulting in convergence errors beyond strand yield.

Other methods for prestressed concrete using another popular high-fidelity structural analysis software program contain simplifying assumptions similar to the method presented by Bojanowski and Balcerzak.¹ A complete deflection history until failure (for example, a compression strain of 0.003) has not yet been demonstrated in this other software program or validated against experimental data, although the potential to do so may exist.² However, convergence errors also appear to be common shortly after the strands exceed their elastic limit.³⁻⁵

More accurate methods for pretensioning have been demonstrated by Yapar et al.⁶ and Schwer.⁷ Yapar et al. modeled the prestressing strands using tetrahedron elements, while Schwer used beam elements. Although the Yapar et al. method is potentially more accurate, it is more computationally costly. In addition, Yapar et al. acknowledge geometric simplifications in their method relating to strand cross-sectional geometries that may negate much of the improved accuracy. Therefore, the Schwer method was faithfully executed in this paper. Qian⁸ used this method to estimate the disproportionate

collapse capacity of a continuous post-tensioned beam under a column-loss scenario. Complete force-deflection responses of well-behaved beams have not yet been investigated or validated against experimental data.

Test plan

Four pretensioned beam geometries were modeled. Physical tests were also performed for all cases as a comparison and to validate the analytical models. **Table 1** shows a test matrix for both the computer model and the laboratory test program. The prestressing forces provided in the table are the sum of all strand forces at the time of testing, which includes reductions due to shrinkage, creep, relaxation, and elastic shortening. The concrete strengths provided in the table are values measured at the time of testing. The concrete's elastic modulus values will be discussed in the following section.

Beam configurations 1, 3, and 4 were designed to optimize the load-bearing capacity relative to self-weight while satisfying the constraints provided by in recent years for the PCI Engineering Student Design Competition, or Big Beam Contest, which define the loading, precrack capacity, and capacity at failure. This explains the unconventional geometries in configurations 3 and 4 (such as high slenderness and aggressive tapering) and the use of high-strength concrete.

Beam configuration 2 is a supplemental test that was conducted to further validate the finite element analysis methodology. All beams were designed to exhibit a limit state of concrete crushing at the top outermost fiber at midspan, well after strand yield.

Finite element analysis

Concrete model

All concrete was modeled using standard hexahedron elements. All steel was modeled using beam elements with an elastic-perfectly plastic material model. The inputs for the prestressing strands were 29,000 ksi (200 GPa) for elastic

Table 1. Test matrix for laboratory testing and computer simulation

Beam configuration number	Loading	Cross-section shape	Span, ft	Total depth, in.	Self-weight, kip	Prestressing force, kip	Concrete strength, ksi	Prestressing strand yield, ksi
1	Three point	I	15	19.5	1.57	69.4	11.0	243
2	Four point	Rectangle	13.5	8	0.47	28.6	13.0	243
3	Four point	Tapered I	18	12 to 19.5	0.73	63.2	18.0	243
4	Six point	Tapered I	20	9 to 16.5	0.83	63.6	17.3	243

Note: 1 in. = 25.4 mm; 1 ft = 0.305 m; 1 kip = 4.448 kN; 1 ksi = 6.895 MPa.

modulus and 243 ksi (1675 MPa) for yield stress. All nodes in the beam elements coincide exactly with concrete nodes, resulting in a “perfect” bond. Rollers, loading pads, and the like, were modeled with hexahedron elements and an elastic material model. Standard contacts were used with appropriate coefficients of static friction.

The *MAT_85 Winfrith concrete model was chosen as the material model.⁹ The fracture energy parameter, which determines crack propagation behavior, was calculated per Bruhl et al.¹⁰ using Eq. (1):

$$\omega = 1.0376 \frac{\phi^{0.32}}{\sqrt{f'_c}} \quad (1)$$

where

ω = crack width at which crack-normal tensile stress goes to zero

ϕ = aggregate diameter in inches

f'_c = concrete unconfined uniaxial compression strength in psi of a 4 × 8 in. (101.6 × 203.2 mm) cylinder

Table 2 lists the concrete mechanical properties that were used in the Winfrith concrete model for each of the beam configurations, namely the following:

- Poisson’s ratio ν
- unconfined compression strength ucs
- tensile strength f_t
- crack width ω
- aggregate radius $asize$

Elastic modulus E was measured at the time of testing. Although Bruhl et al.¹⁰ use $2.5\sqrt{f'_c}$ for the Winfrith tensile strength parameter f_t and Schwer¹¹ uses the cube strength for the unconfined compression strength ucs (Table 2), reliable and accurate simulation results were achieved using $7.5\sqrt{f'_c}$ for f_t and f'_c for ucs . The Winfrith model would not be able to

simulate beam configuration 3 if the cube strength were used because the current form of the Winfrith model cannot handle ucs values in excess of 21 ksi (145 MPa).

The loading was performed using displacement control. Because the Winfrith model is currently incompatible with implicit time integration, explicit time integration was used. To reduce computational cost, the concrete density was artificially increased (mass scaling) and the loading rate was set to an artificially fast 1.33 in./sec (33.8 mm/sec). Sensitivity studies were performed to ensure a proper balance of cost with loading rate, mesh size, and sampling rate. Symmetry conditions were not employed because the most computationally costly beam run consisted of rollers and pads in the loading tree that were placed in an asymmetric fashion. In addition, in order to permit lateral-torsional buckling, the concrete beams were left unrestrained in the out-plane direction except for the friction provided to the top flange from the loading apparatus.

Model simulations

Three simulations were performed for each beam configuration, identified as phases 1, 2, and 3. During phase 1, the prestressing strands were tensioned by themselves. Just as strand tensioning is performed in a pretensioning bed at the prestressing plant before the concrete placement (**Fig. 1**), the concrete was absent during this phase in the computer model. In addition, to maintain the harped-strand profile, hold-downs are used in the pretensioning bed, which must be present in the computer model as well. In the model, vertical boundary conditions were used at the locations of the hold-downs.

In the computer model, *LOAD NODE is used at the nodes at the extreme ends of the beam to introduce the prestressing axial force in the strands (for example, 27.3 kip [121.4 kN] into each of the two bottom strands for beam configuration 3). The program ramps up the load over a short period of time using a dynamic relaxation approach. **Figure 1** shows that a constant axial force was present in the strands along their lengths at the end of phase 1. Once the phase 1 simulation was complete, the steel stresses were exported to a text file. The sole purpose of phase 1 was to obtain this text file.

In the fabrication process at a prestressing plant, the concrete

Table 2. Winfrith concrete model relevant concrete properties

Beam configuration number	Elastic modulus E , ksi	Poisson’s ratio ν	Unconfined compression strength ucs , ksi	Winfrith tensile strength parameter f_t , ksi	Crack width ω , in.	Aggregate radius $asize$, in.
1	4000	0.18	11.0	0.790	0.007290	0.1925
2	5520	0.18	13.0	0.850	0.006680	0.1875
3	6040	0.18	18.0	1.010	0.005650	0.1875
4	6100	0.18	17.3	0.990	0.005764	0.1875

Note: ω = crack width at which crack-normal tensile stress goes to zero. 1 in. = 25.4 mm; 1 ksi = 6.895 MPa.



Prestressed Beam Test
 Time = 0
 Contours of Axial Force
 min=-0.120001, at elem# 1761
 max=27307, at elem# 313

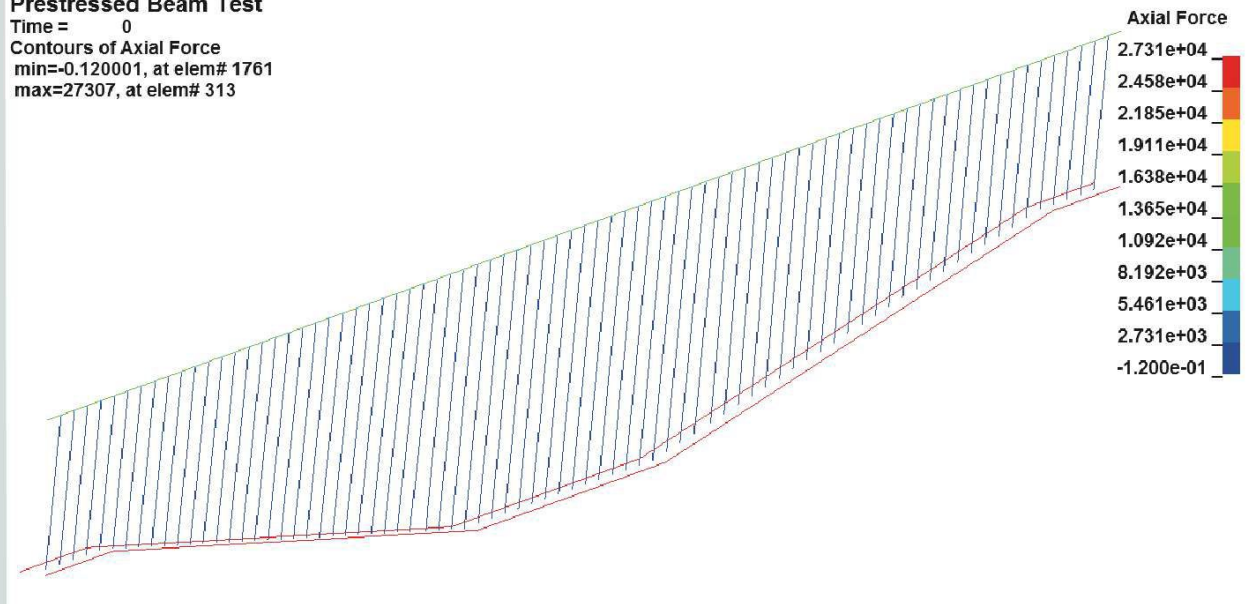


Figure 1. Pretensioned strands ready for concrete placement (top) and simulation of pretensioning (bottom) for beam configuration 3. Note: Force values are in pounds. elem# = element number; max = maximum; min = minimum. 1 lb = 4.448 N. Photo courtesy of Blakeslee Prestress Inc.

would then be placed and given time to cure and to bond to the prestressing strands, and then the strands would be cut, which puts the concrete into its compressive prestressed state. Phase 2 simulates this intermediate stage, where the concrete is prestressed without application of any other external forces.

In the computer model, the text file from phase 1 is used as input for phase 2. In phase 2, the boundary conditions on the strands that represented hold-down anchors were removed and the concrete was then present. **Figure 2** shows the concrete compression resulting from phase 2. The beam was then prestressed.

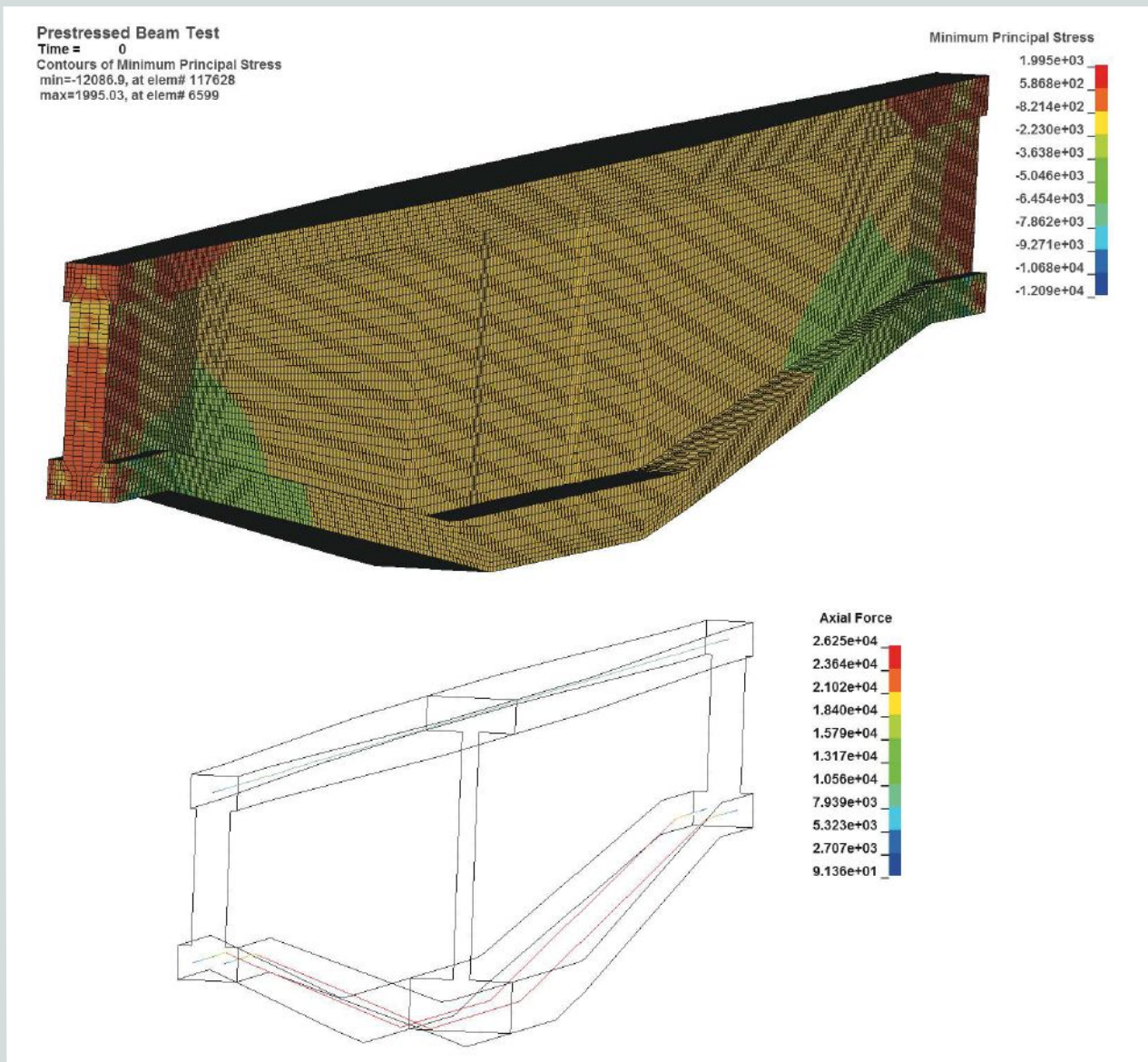


Figure 2. Concrete prestressed from strands (top) and strand loss of force due to development and concrete elastic shortening for beam configuration 3 (bottom). Note: Force values are in pounds. Stress values are in pounds per square inch. elem# = element number; max = maximum; min = minimum. 1 lb = 4.448 N; 1 psi = 6.895 kPa.

In addition, due to elastic shortening, the forces in the prestressing strands were somewhat reduced, compared with the forces that were present in phase 1. Figure 2 shows the new strand forces, which were indeed smaller and also no longer constant along their length. Once the phase 2 simulation was complete, the steel and concrete stresses were exported to a text file. The sole purpose of phase 2 was to obtain this new text file.

In the computer model, the text file from phase 2 was used as input for phase 3. Phase 3 was performed using an explicit dynamic analysis and was the final phase, which in this case vertically loaded the beam until failure.

In the computer model, the loading was applied in the same way as in the actual experiment. **Figure 3** shows, for example, that bearing pads applied the load to the concrete beam

and that friction prevented the pads from sliding as the beam deflected. In this particular beam configuration (configuration 3), a steel wide-flange spreader beam was used to apply the load to two small rollers that in turn applied the load to the aforementioned bearing pads.

Figure 4 depicts the contacts that were present in the computer model and also highlights the nodes at the top of the small rollers (on top of the concrete beam) where the displacement control was applied. Boundary conditions (not shown) were present on the nodes at the bottom of the large rollers (beneath the concrete beam) as well.

Results

Table 3 summarizes the results for each of the beam configu-



Figure 3. Experimental test setup with steel spreader beam, rollers, and pads for beam configuration 3.

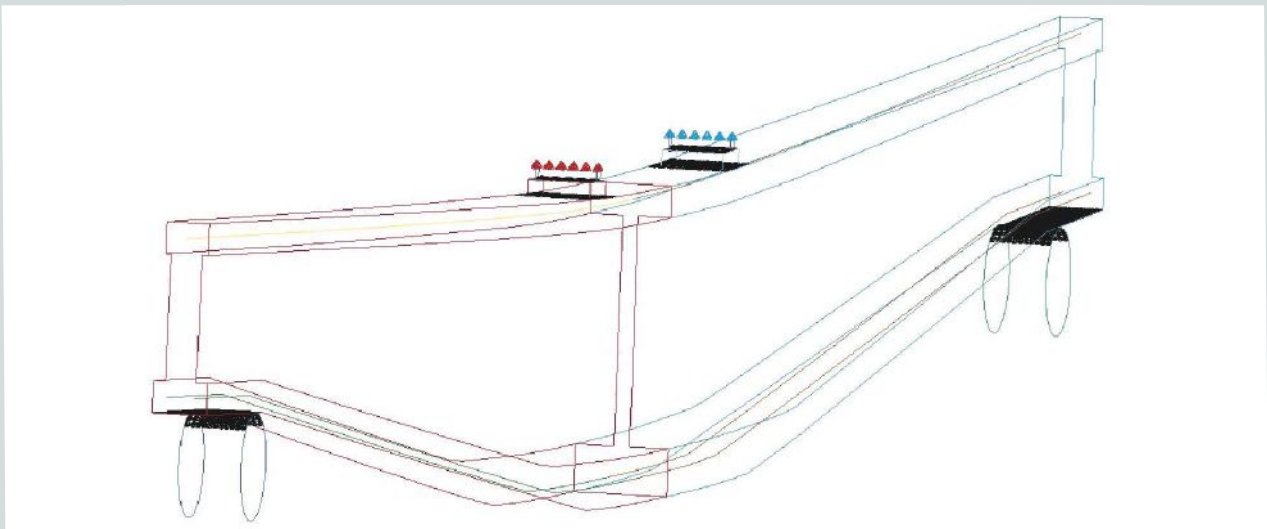


Figure 4. Contact surfaces and loaded nodes for beam configuration 3.

Table 3. Predicted and experimental program results

Beam configuration number	Computational cost, CPU hours	Experimental deflection, in.	Predicted force, kip	Experimental force, kip	Error, %
1	1280	0.77	40.5	38.5	5
2	384	2.16	6.45	6.08	6
3	2176	3.48	35.4	35.7	1
4	2560	6.10	34.1	33.1	3

Note: CPU = central processing unit. 1 in. = 25.4 mm; 1 kip = 4.448 kN.

rations for the finite element analysis and physical laboratory testing. The forces in Table 3 correspond to the total applied force on each beam at a particular value of measured deflection. For consistency, the deflection value used was taken to be the deflection at the instant that the top outermost fiber at midspan was $-2500 \mu\epsilon$. For experimental tests, strains and deflections were measured using strain gauges and string potentiometers placed at midspan. The total applied force was taken directly from the load output from the test apparatus.

The value of $-2500 \mu\epsilon$ was chosen because a strain of $-3000 \mu\epsilon$ for unconfined concrete indicates imminent failure and the beams were designed so that the prestressing strands began to yield when the concrete compression reached approximately $-1500 \mu\epsilon$. Therefore, $-2500 \mu\epsilon$ is an appropriate intermediate value. The force and deflection values as well as computational cost (runtime multiplied by processors) are shown in Table 3.

Figures 5 and 6 show screenshots from the software program along with force-deflection plots for each of the four beam configurations. The plots show that each beam exhibited three regions of behavior:

- a region in which the concrete remained elastic
- a region in which the concrete cracked but the prestressing strands remained elastic
- a region in which the strands yielded

The screenshots in Fig. 5 and 6 show that the Winfrith model was able to predict the crack pattern, which was calculated using ω , the crack width at which crack-normal tensile stress goes to zero, from Eq. (1). This crack pattern was generally quite close to the crack pattern observed in the tests. For example, with beam configuration 2, predicted results (Fig. 5) and experimental results (**Fig. 7**) show nearly identical crack patterns. This was true for every beam configuration. In Fig. 7, the string potentiometer is connected with a zip tie to the top midspan of the beam. The abrupt jumps in the simulation data correspond to the release of energy when each crack formed, which occurred more rapidly in the simulations compared with the physical experiments. The reason these jumps were not present in the experimental plots is the slow rate of crack propagation due to the slow loading rate in the experiments. Replicating the exact loading rate of tests would have been too computationally costly to simulate.

Practical application

The prediction of the response of a prestressed beam or system of prestressed beams to extreme loads, such as impact or blast, is an example of where high-fidelity computer simulations would be used. To demonstrate, **Fig. 8** shows the response of a concrete slab to a dynamic blast load. The blast load applied was an impulsive load of approximately 50 psi (344.75 kPa) over a duration of approximately 25 milliseconds. This slab was supported by a system of five pre-

sioned beams. Figure 8 shows a screenshot from the simulation as the deflection approached its peak at 90 milliseconds.

In this structure, the prestressed beam model from beam configuration 1 was used for each of the five beams. The choice to use beam configuration 1 rather than another beam configuration was an arbitrary choice. Phases 1 and 2 for this particular beam were unchanged, as were the corresponding text file stresses. Thus, the phase 3 model, which was the self-contained pretensioned beam, was simply placed underneath the reinforced concrete slab and replicated four additional times to generate the five pretensioned beams supporting the reinforced concrete slab.

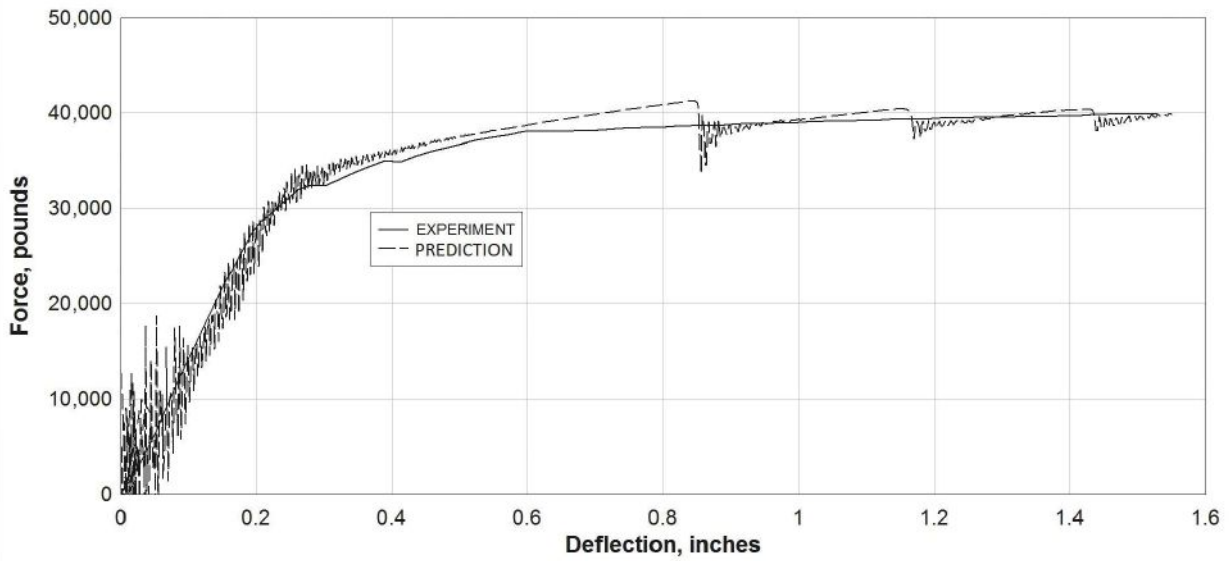
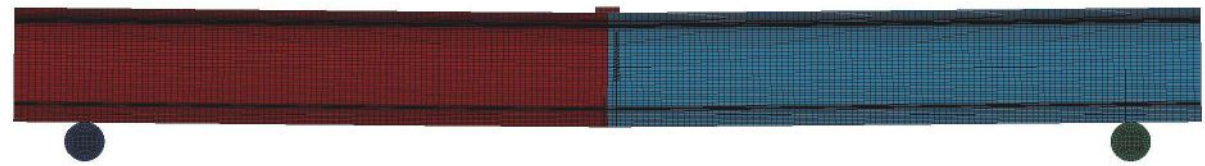
If the termination time for this blast simulation is set to 90 milliseconds to capture the peak deflection, then the computational cost is about half of the cost of the quasistatic, displacement-controlled simulation for a single beam (Table 3). More information on the structural slab and wall geometry used for this blast simulation, as well as deflection-time histories for similar blast tests, additional general context, and additional material validation are provided in Drummond.¹² Thus, it is demonstrated that the previously outlined pretensioning method, along with the Winfrith concrete material model, can be easily extended to practical applications and high-performance computers are often not needed for such applications.

Conclusion

The ability to accurately predict the entire force-deflection behavior of prestressed concrete structures will facilitate the analysis of extreme load response and/or structures of complex geometries. As computational power perpetually increases and high-fidelity structural analysis becomes more common, these analysis methodologies will likely become more user friendly and the software more accessible.

- A methodology from Schwer⁷ was reviewed. The methodology uses a software program to model the structural response of prestressed concrete in three stages, starting with the prestressing strands with the concrete absent, followed by equilibrium between the strands and the rest of the structure upon placement of the concrete. Once equilibrium is achieved at this intermediate stage, loads are applied to the composite steel/concrete structure in a manner identical to any typical high-fidelity finite element analysis.
- Force variation within the strand at the pretensioning stage is captured in the simulation.
- The entire load-deflection history up to concrete crushing failure is captured in the simulation. This includes the elastic concrete regime, cracked concrete (with elastic strands), and the postyielding regime.
- The ability of this method to predict pretensioned con-

Beam Configuration 1



Beam Configuration 2

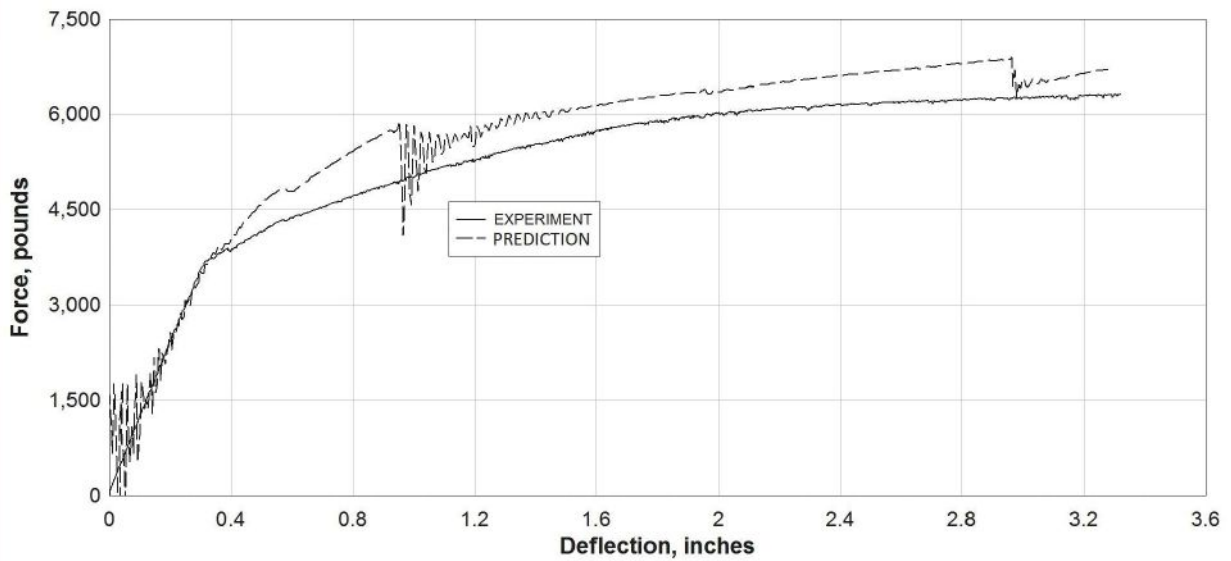
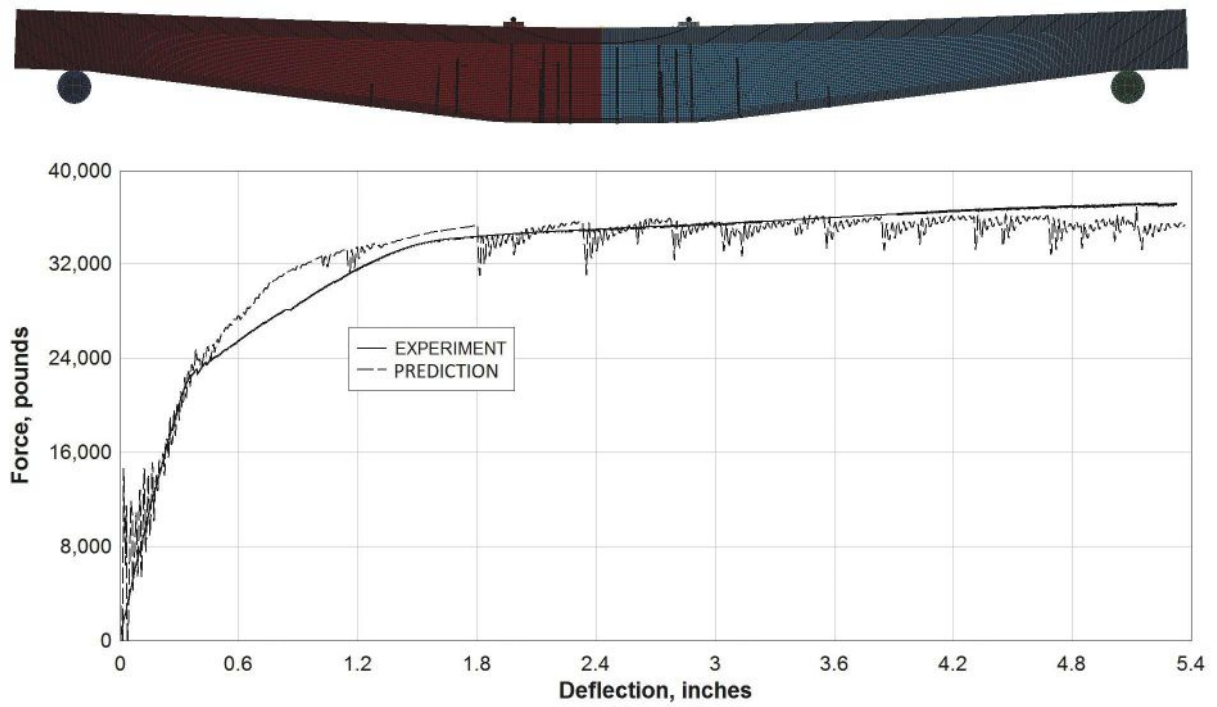


Figure 5. Experimental and predicted forces versus deflection for beam configurations 1 and 2. Note: 1 in. = 25.4 mm; 1 lb = 4.448 N.

Beam Configuration 3



Beam Configuration 4

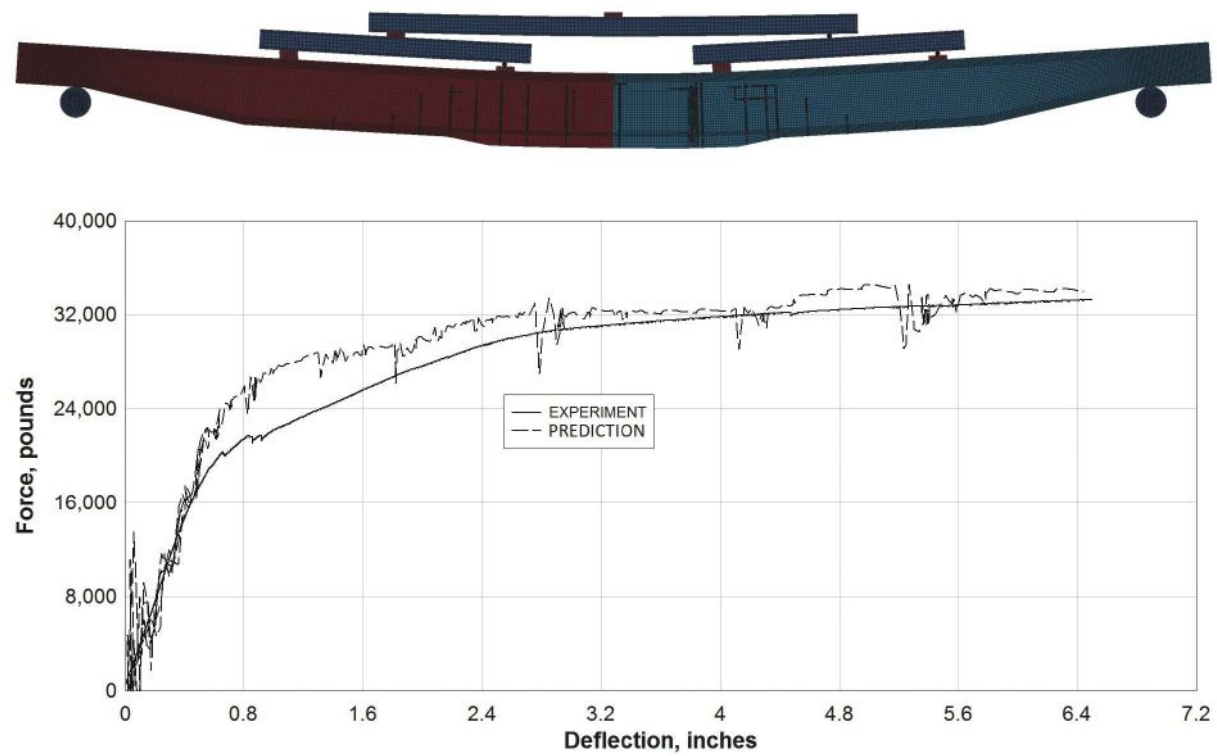


Figure 6. Experimental and predicted forces versus deflection for beam configurations 3 and 4. Note: 1 in. = 25.4 mm; 1 lb = 4.448 N.



Figure 7. Crack pattern during beam configuration 2 experiment.

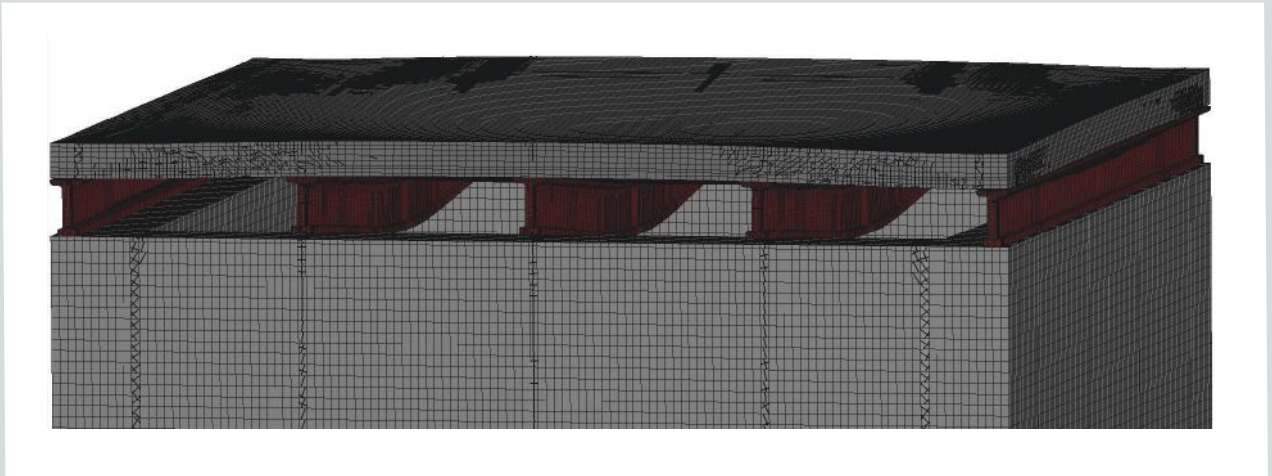


Figure 8. Prestressed structure response to blast loading.

crete beam behavior was demonstrated on four beams of widely differing geometries and material properties using a displacement-controlled explicit dynamic approach. By comparison against experimental data, the accuracy of each of the finite element analysis simulations was validated, with a maximum force versus deflection error of 6%.

- The Winfrith concrete material model was used. The

model has the unique ability to display crack propagations, allowing qualitative validation.⁸

- Finally, a practical example of a blast simulation was shown.

Acknowledgments

The authors would like to acknowledge useful discussions

with Jake Bruhl, Len Schwer, Nathan Pauls, Robert Drummond, and Andrew Valkenburg. We would also like to acknowledge the assistance with data acquisition from Eric Horne and the expertise of Robert Vitelli and Rick Fitzgerald of Blakeslee Prestress Inc. for the concrete mixture proportions and beam casting. All beams were constructed and donated by Blakeslee Prestress Inc. The high-fidelity simulations were performed using U.S. Department of Defense High Performance Computing Modernization Program systems. Plans, elevations, cross-sectional geometries, reinforcing steel and strand information, load locations, and computer model information will be shared by the authors upon request.

References

1. Bojanowski, C., and M. Balcerzak. 2014. "Response of a Large Span Stay Cable Bridge to Blast Loading." Paper presented at 13th International LS-DYNA Users Conference, Dearborn, MI, June 2014.
2. Hawileh, R. A., A. Rahman, and H. Tabatabai. 2010. "Nonlinear Finite Element Analysis and Modeling of a Precast Hybrid Beam-Column Connection Subjected to Cyclic Loads." *Applied Mathematical Modelling* 34 (9): 2562–2583.
3. Fanning, P. 2001. "Nonlinear Models of Reinforced and Post-Tensioned Concrete Beams." *Electronic Journal of Structural Engineering* 2: 111–119.
4. Wolanski, A. J. 2004. "Flexural Behavior of Reinforced and Prestressed Concrete Beams Using Finite Element Analysis." MS thesis, Marquette University, Milwaukee, WI.
5. Joshua, N. R., S. Saibabu, P. Eapen Sakaria, K. N. Lakshmikandhan, and P. Sivakumar. 2014. "Finite Element Analysis of Reinforced and Pre-tensioned Concrete Beams." *International Journal of Emerging Technology and Advanced Engineering* 4 (10): 449–457.
6. Yapar, O., P. K. Basu, and N. Nordendale. 2015. "Accurate Finite Element Modeling of Pretensioned Prestressed Concrete Beams." *Engineering Structures* 101: 163–178.
7. Schwer, L. 2016. "Modeling Pre and Post Tensioned Concrete." Paper presented at 14th International LS-DYNA Users Conference, Dearborn, MI, June 2016.
8. Qian, K., Z.-Z. Li, F.-X. Cen, and B. Li. 2018. "Strengthening RC Frames against Disproportionate Collapse by Post-tensioning Strands." In *Structures Congress 2018: Blast, Impact Loading, and Response; and Research and Education*. J. G. Soules, ed. Reston, VA: American Society of Civil Engineers.
9. Broadhouse, B. J. 1995. "The Winfrith Concrete Model in LS-DYNA3D." SPD/D(95)363. AEA Technology,

Winfrith Technology Centre. https://ftp.lstc.com/anonymous/outgoing/jday/concrete/Winfrith_Paper_Feb1995.pdf.

10. Bruhl, J. C., A. H. Varma, and J. M. Kim. 2015. "Static Resistance Function for Steel-Plate Composite (SC) Walls Subject to Impactive Loading." *Nuclear Engineering and Design* 295: 843–859.
11. Schwer, L. 2011. "The Winfrith Concrete Model: Beauty or Beast? Insights into the Winfrith Concrete Model." Paper presented at 8th European LS-DYNA Users Conference, Strasbourg, France, May 2011.
12. Drummond, R., C. Sun, A. Valkenburg, A. Freidenberg, and J. C. Bruhl. 2019. "Computer Predictions of Tunnel Response to Blast." In *Structures Congress 2019: Blast, Impact Loading, and Research and Education*, edited by James Gregory Soules, 31–47. Reston, VA: American Society of Civil Engineers.

Notation

a_{size}	= aggregate radius
E	= elastic modulus
f'_c	= concrete unconfined uniaxial compression strength of a 4 × 8 in. (10.16 × 20.32 cm) cylinder
f_t	= Winfrith tensile strength parameter
uc_s	= unconfined compression strength
ν	= Poisson's ratio
ϕ	= aggregate diameter
ω	= crack width at which crack-normal tensile stress goes to zero

About the authors



Aaron Freidenberg is an assistant professor in the Department of Civil and Mechanical Engineering at the U.S. Military Academy in West Point, N.Y. His research interests are related to investigating the response of structures to extreme loads using high-performance computing. His PhD research at University of California, San Diego, involved dynamic loading experiments using the Extreme Events Simulator.



Lyle R. Milliman, PE, is an assistant professor in the Civil and Mechanical Engineering Department at the U.S. Military Academy, where he works with cadets on reinforced concrete and prestressed concrete design. He is an active duty army officer in the Army Corps of Engineers, with combat deployments to Iraq and Afghanistan. He obtained his bachelor of science degree from the United States Military Academy, West Point, in 2006 and his master of science degree from the University of Wisconsin-Madison in 2015.



Ben Parmer received his bachelor of science degree from the Department of Civil and Mechanical Engineering at the U.S. Military Academy in 2018. He was a member of the two-person 2018 PCI Big Beam team at the U.S. Military Academy.



Gbenga M. Olaolorun is an active duty army officer in the Nigerian Army Engineers, where he performs both military and civil engineering tasks. He obtained his bachelor of science degree in civil engineering from the U.S. Military Academy in 2017. While at the U.S. Military Academy, he developed an interest in concrete design, which prompted him to participate in the international PCI capstone project on prestressed concrete structures.



Evan Pape received his bachelor of science degree from the Department of Civil and Mechanical Engineering at the U.S. Military Academy in 2018. He was a member of the two-person 2018 PCI Big Beam team at the U.S. Military Academy.



Brad Durant is a research structural engineer in the Explosion Effects and Consequences division at NAVFAC Engineering and Expeditionary Warfare Center in Port Hueneme, Calif. His focus areas include analysis of blast effects and protective construction for explosives safety compliance and the response of structures to extreme loading conditions. He conducted his graduate research at University of California, San Diego, under the Air Force Research Laboratory Munitions Directorate and has overseen the design and development of multiple blast-resistant portable buildings.

Abstract

Structural behavior of pretensioned concrete beams can be difficult to predict. For example, deflections of pretensioned concrete beams are difficult to predict analytically but are sometimes needed for serviceability or construction considerations. A prestressed concrete beam's response to dynamic loads or under extreme loads, such as blast, are also difficult to predict. Prestressed concrete structures other than slender beams present yet another challenge. A high-fidelity finite element analysis approach is reviewed in this paper, and it can be used to predict the entire dynamic response up to failure for pretensioned concrete structures of any geometry under any loading. To demonstrate this computational method, four pretensioned concrete beams of varying geometries were loaded quasistatically well beyond the elastic regime of both the concrete and the steel prestressing strands and the analytical results were compared with experimental results. The method is described in detail, and the deflections and strains from the simulations (including visualization of cracks) from the simulations are compared with the test data. It is demonstrated that the computer models are able to predict the entire load deflection response within a maximum error of 6%. Qualitative results, namely crack patterns, are compared as well.

Keywords

Blast, finite element analysis, pretensioned, simulation, Winfrith model.

Review policy

This paper was reviewed in accordance with the Precast/Prestressed Concrete Institute's peer-review process.

Reader comments

Please address any reader comments to *PCI Journal* editor-in-chief Emily Lorenz at elorenz@pci.org or Precast/Prestressed Concrete Institute, c/o *PCI Journal*, 200 W. Adams St., Suite 2100, Chicago, IL 60606. [▶](#)